

# Reversible Photocontrollable Magnetic Vesicles Consisting of Azobenzene

Yasuaki Einaga,<sup>\*,†</sup> Takashi Yamamoto,<sup>†</sup> Takeshi Sugai,<sup>†</sup> and Osamu Sato<sup>‡</sup>

Department of Chemistry, Faculty of Science and Technology, Keio University, 3-14-1 Hiyoshi, Yokohama 223-8522, Japan, and Kanagawa Academy of Science and Technology, KSP, 3-2-1 Sakado, Kawasaki 213-0012, Japan

Received July 2, 2002. Revised Manuscript Received September 27, 2002

Photochromic magnetic vesicles have been designed by intercalation of Prussian blue into a lipid bilayer membrane which consists of azobenzene. Reversible photoisomerization of the solid system realized reversible photocontrol of the magnetic properties. Here, we have synthesized an amphiphile azo moiety containing a long alkyl chain, and we have prepared photochromic magnetic vesicles consisting of only this azo moiety. As a result, the magnetic property change brought about by visible light illumination was estimated to be ca. 13%, which is much larger than the figure achieved for the similar system that we reported previously (~1%), which contained the double-chain ammonium amphiphile (*J. Am. Chem. Soc.* **1999**, *121*, 3745).

## Introduction

Reversible phototunable magnetic systems, including spin crossover compounds, have attracted much attention in recent years.<sup>1,2</sup> The incorporation of organic photochromes into magnetic systems is of topical interest as a possible new strategy for realizing such a system.<sup>3–10</sup> In this technique, the photoisomerization of photochromic compounds accompanied by geometric and electronic structural changes can be used to control the magnetic properties of the composite materials.

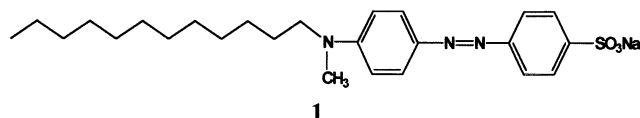
In our previous work, we have reported an example of such an inorganic/organic composite material comprising of Prussian blue intercalated into photoresponsive organic molecules (azobenzene-containing multibilayer vesicles).<sup>7</sup> Although this was the first known example of photocontrollable magnetic vesicles, the degree of photocontrol of the magnetization value, which was accompanied by *cis*–*trans* photoisomerization, was

very small (~1%). It has been suggested that this is because structural changes to the vesicles, which induce the change in dipole moment and electrostatic field, were relatively small. That is, the photofunctional vesicles consist not only of the azo moiety, but also the dialkylammonium amphiphile in order to form the spherical vesicles.

For the work reported herein, we have synthesized spherically closed amphiphilic bilayers containing the azo moiety, and have designed a photofunctional composite system with Prussian blue in the poly(vinyl alcohol) (PVA) matrix films.

## Experimental Section

**Preparation of the Composite Film.** An amphiphilic azo compound **1**, 4-[4-(*N*-methyl-*N*-dodecylamino)phenylazo]benzenesulfonic acid, sodium salt, was synthesized according to a procedure reported in the literature.<sup>11</sup>



A photoisomerizable composite film was prepared using the same method as in our previous work.<sup>7</sup> Briefly, a sonicated clear solution containing amphiphiles **1** (5 mM) was prepared in deionized H<sub>2</sub>O, and this dispersion was mixed with an aqueous solution of poly(vinyl alcohol) (PVA, MW ≈ 70 000, 200 mg; H<sub>2</sub>O, 4 mL). PVA acts as a matrix for **1** (mixing weight ratio, **1**/PVA = 1:20). The composite film, hereafter designated film **2** (= **1** + PVA), was prepared by casting the above solution onto a clean glass plate (pretreated with concentrated sulfuric acid) at room temperature.

**Intercalation.** Prussian blue, a molecule-based magnetic compound, was intercalated. The method used for this is also the same as that used in our previous work, although the

- \* To whom correspondence should be addressed. Phone: 81-45-566-1704. Fax: 81-45-566-1697. E-mail: einaga@chem.keio.ac.jp.
- † Keio University.
- ‡ Kanagawa Academy of Science and Technology.
- (1) Letard, J.-F.; Real, J. A.; Moliner, N.; Gaspar, A. B.; Capes, L.; Cador, O.; Kahn, O. *J. Am. Chem. Soc.* **1999**, *121*, 10630.
- (2) (a) Sato, O.; Iyoda, T.; Fujishima, A.; Hashimoto, K. *Science* **1996**, *272*, 704. (b) Sato, O.; Einaga, Y.; Iyoda, T.; Fujishima, A.; Hashimoto, K. *J. Electrochem. Soc.* **1997**, *144*, L11. (c) Sato, O.; Einaga, Y.; Fujishima, A.; Hashimoto, K. *Inorg. Chem.* **1999**, *38*, 4405. (d) Hayami, S.; Gu, Z.-Z.; Shiro, M.; Einaga, Y.; Fujishima, A.; Sato, O. *J. Am. Chem. Soc.* **2000**, *122*, 7126. (e) Gütlich, P.; Garcia, Y.; Woike, T. *Coord. Chem. Rev.* **2001**, *219*–*221*, 839.
- (3) Fendler, J. H. *Chem. Rev.* **1987**, *87*, 877.
- (4) Irie, M. *Chem. Rev.* **2000**, *100*, 1685.
- (5) Berkovic, G.; Krongauz, V.; Weiss, V. *Chem. Rev.* **2000**, *100*, 1741.
- (6) Nakatani, K.; Yu, P. *Adv. Mater.* **2001**, *13*, 1411.
- (7) Einaga, Y.; Sato, O.; Iyoda, T.; Fujishima, A.; Hashimoto, K. *J. Am. Chem. Soc.* **1999**, *121*, 3745.
- (8) Einaga, Y.; Gu, Z.-Z.; Hayami, S.; Fujishima, A.; Sato, O. *Thin Solid Films* **2000**, *374*, 109.
- (9) Benard, S.; Yu, P. *Adv. Mater.* **2000**, *12*, 48.
- (10) Benard, S.; Riviere, E.; Yu, P.; Nakatani, K.; Delouis, J. F. *Chem. Mater.* **2001**, *13*, 159.

- (11) Kunitake, T.; Okahata, Y.; Shimomura, M.; Yasunami, S.; Takarabe, K. *J. Am. Chem. Soc.* **1981**, *103*, 5401.

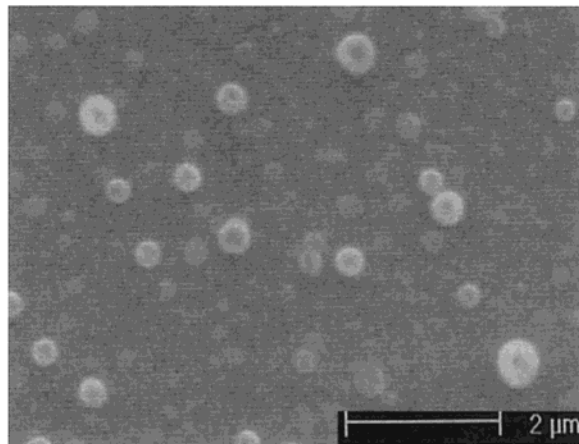
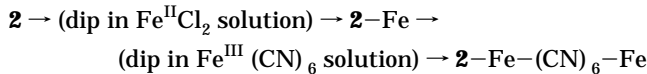


**Figure 1.** SEM image of **2**. A 0.5% aqueous solution of RuO<sub>4</sub> was used to stain the vesicles and improve their visibility.

actual stepwise order was different from the previous scheme. Briefly **2**–Fe–(CN)<sub>6</sub>–Fe was prepared by a procedure as follows:



A sample of cast film **2** was immersed in an aqueous solution of Fe<sup>II</sup>Cl<sub>2</sub> (50 mM) for several hours at room temperature to enable cation exchange with the sodium ion. After being washed with deionized H<sub>2</sub>O, the sample went into suspension as an aqueous gel, which was recast on a clean glass plate (**2**–Fe). To prepare the Fe–CN–Fe framework, the **2**–Fe film was next immersed in an aqueous solution of K<sub>3</sub>Fe<sup>III</sup>(CN)<sub>6</sub> solution (50 mM) for several hours at room temperature. After being washed thoroughly with deionized H<sub>2</sub>O, it was kept in H<sub>2</sub>O for several hours to remove unreacted [Fe<sup>III</sup>(CN)<sub>6</sub>]<sup>3-</sup> ion (**2**–Fe–(CN)<sub>6</sub>–Fe).

**Physical Method.** An ultrasonicator (Sonic and Materials, model VCX-750) was used (200 W, 30 min) to prepare a clear solution containing amphiphiles. A scanning electron micro-

scope (SEM, model XL30, NIKON Intec) was used to image the amphiphiles, and the local chemical compositions of the samples were obtained using an energy-dispersive X-ray spectrometer (EDX). To enhance their visibility, the amphiphiles were stained with a 0.5% aqueous solution of RuO<sub>4</sub>. The magnetic properties were investigated with a superconducting quantum interference device (SQUID) magnetometer (model MPMS-5S, Quantum Design). UV–visible absorption spectra were recorded on a V-560 spectrophotometer (Jasco). The UV–vis measurements at low temperature were performed with a closed-cycle helium refrigerator (Iwatani Co., Ltd.). UV illumination (filtered light,  $\lambda_{\text{max}} = 360 \text{ nm}$ , 1.0 mW/cm<sup>2</sup>) was carried out using an ultrahigh-pressure mercury lamp (Hypercure 200, Yamashita Denso). Similarly, visible light illumination (400–700 nm, 1.0 mW/cm<sup>2</sup>) was carried out using a xenon lamp (XFL-300, Yamashita Denso).

## Results and Discussion

**Films of Photoisomerizable Vesicles.** A scanning electron micrograph (SEM) image of film **2** (= **1** + PVA) indicates the presence of ring-like and spheroidal objects of heterogeneous diameters (diam. 500 nm; Figure 1). More so, a cast film of **1** exhibited a series of X-ray diffraction patterns that correspond to a long-range spacing of 50.7 Å up to the 4<sup>th</sup> order (Figure 2a).

Photoisomerization of film **2** was monitored by UV–vis absorption spectroscopy. The typical UV–vis spectral changes due to the photoisomerization process are shown in Figure 3. Before illumination, the film consisted of only the trans form of the azo compound, because this isomer is thermodynamically more stable than the cis form.<sup>12</sup> By illumination with visible light at room temperature of the trans isomer, some of the trans isomers were converted to the cis isomer (process (i) in Figure 3a). The peak at around 450 nm decreased, whereas the peak at around 360 nm increased. The 450- and 360-nm peaks are ascribed to the  $\pi-\pi^*$  transitions of the trans and cis isomers, respectively. Normally, the trans–cis isomerization is affected by illumination of

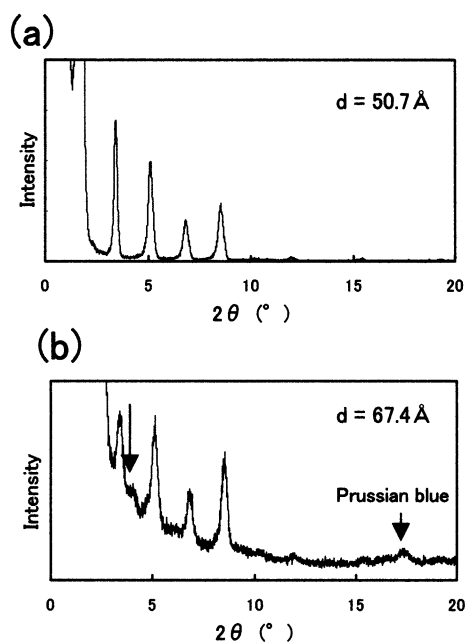
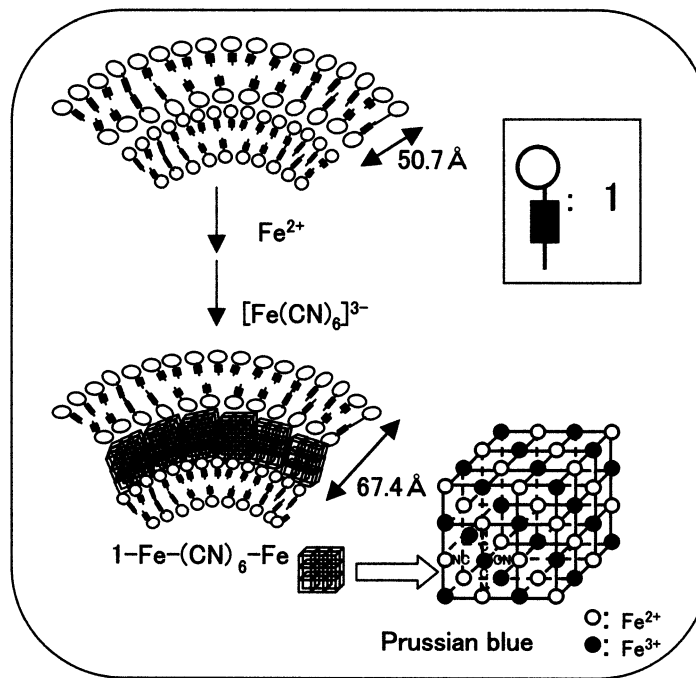


**Figure 2.** Schematic illustration of the stepwise synthesis of **1**–Fe–(CN)<sub>6</sub>–Fe. The XRD patterns of (a) **1** and (b) **1**–Fe–(CN)<sub>6</sub>–Fe are shown on the right. The arrows show new peaks after the intercalation of Prussian blue.  $2\theta = 17.5^\circ$  (5.1 Å) is ascribed to the Fe<sup>II</sup>–CN–Fe<sup>III</sup> framework in the film. **2**–Fe–(CN)<sub>6</sub>–Fe contains **1**–Fe–(CN)<sub>6</sub>–Fe and PVA, which acts as a matrix.

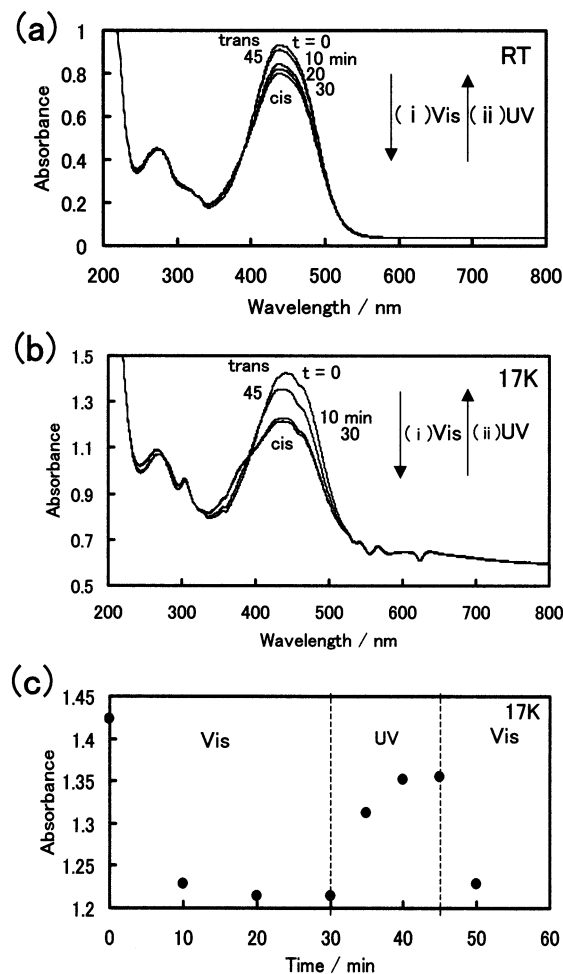


**Figure 3.** Changes in the optical absorption spectra due to photoisomerization for film **2**. (a) The initial trans state was first illuminated at room temperature with visible light (400–700 nm, 100 mW/cm<sup>2</sup>) for 30 min. Spectra were recorded every 10 min during the illumination. Then, the isomerized cis state was illuminated with UV light (360 nm, 100 mW/cm<sup>2</sup>) for 15 min. The spectrum at time  $t = 45$  min (after 30 min of visible illumination followed by 15 min of UV illumination) was almost identical to that before illumination ( $t = 0$ ). (b) At 17 K, the same measurements as those at room temperature were performed. The spectrum at time  $t = 45$  min (after 30 min of visible illumination followed by 15 min of UV illumination) showed that the trans-to-cis photoisomerization proceeded with a conversion efficiency of ca. 70%. (c) Changes in the absorbance at 438 nm at 17 K.

$\pi-\pi^*$  band of the trans isomer, which is in the UV. However, in the film **2**, para-substitution of electron acceptor/donor groups ( $\text{SO}_3\text{Na}$  and  $\text{CH}_3(\text{CH}_2)_{11}\text{N}(\text{CH}_3)$ ) in the basic azobenzene chromophore results in substantial shifts of the  $\pi-\pi^*$  peak in to the visible part of the electromagnetic spectra.<sup>13</sup> The reason the trans-to-cis photoisomerization was not perfect is that the photoisomerization of azobenzene derivatives is accompanied by an increase in molecular volume in this PVA film system. In fact, it is known that the solid-state reaction is greatly inhibited because of close packing of the chromophores.<sup>14</sup> In the present system,

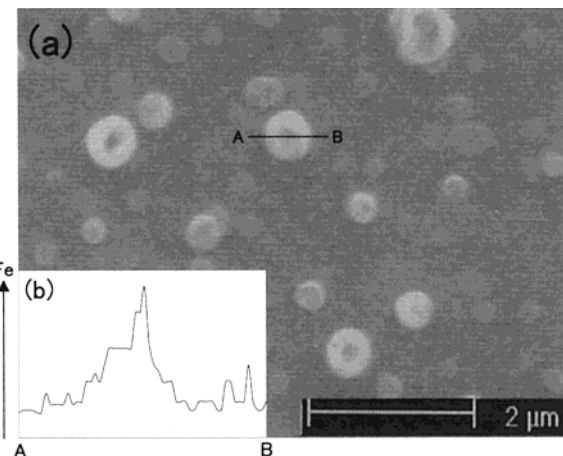


**Figure 4.** (a) SEM image of **2**–Fe–(CN)<sub>6</sub>–Fe. (b) EDX analysis along the line indicated in part (a), showing the relative intensity for Fe along the line (arrow indicates increasing intensity).

the existence of a strong interaction between the chromophores in the vesicle conformation also restricts the photoinduced conformation change to some extent.

After subsequent illumination with UV light, the reverse process, i.e., the cis-to-trans isomerization, proceeded almost completely (process (ii) in Figure 3a). Furthermore, almost the same photoisomerization trend was also observed at low temperature (17 K) (Figure 3b).

**Characterization of the Intercalated Films.** The formation of the  $\text{Fe}^{\text{II}}\text{–CN–Fe}^{\text{III}}$  framework was accomplished by immersing the **2**–Fe film in an aqueous solution of  $\text{K}_3\text{Fe}^{\text{III}}\text{ (CN)}_6$ . Figure 4a shows an SEM image of the resulting film, designated **2**–Fe–(CN)<sub>6</sub>–Fe. The relative amount of Fe in the film was measured using EDX along the line indicated in Figure 4a. This analysis (Figure 4b) suggests that the intercalated Prussian blue exists inside the vesicles, not outside.

The cast film of **1**–Fe–(CN)<sub>6</sub>–Fe exhibited a series of X-ray diffraction patterns that correspond to a long-range spacing of not only 50.7 Å, which corresponds to **1**, but also of 67.4 Å (Figure 2b). Moreover, another diffraction peak at  $2\theta = 17.5^\circ$  (5.1 Å), which is ascribed to the  $\text{Fe}^{\text{II}}\text{–CN–Fe}^{\text{III}}$  framework, was also observed. It has been suggested that the ordered bilayer structure remains intact during complex formation, and that three-layered Prussian blue is intercalated between the bilayer structures. The schematic illustration of the stepwise synthesis was shown in Figure 2.

The UV-vis absorption spectra also suggest the existence of Prussian blue inside the vesicles. The absorption spectrum of the **2**–Fe–(CN)<sub>6</sub>–Fe film revealed a broad peak centered at 680 nm which is related to the internal charge-transfer band from  $\text{Fe}^{\text{II}}$  to  $\text{Fe}^{\text{III}}$ . This absorption maximum,  $\lambda_{\text{max}}$ , is blue-shifted by ca. 20 nm from that of bulk Prussian blue.<sup>15</sup> This suggests that the surface of the  $\mu$ -cyanide complex is in contact with the anionic bilayer surface. The existing electrostatic field will therefore heighten the Coulombic energy necessary for transferring an electron from the hexacyanoferrate (II) ion to the surface Fe (III) species, thus resulting in the blue-shifted absorption spectrum.<sup>16</sup>

(12) Adamson, A. A.; Vogler, A.; Kunkely, H.; Wachter, R. *J. Am. Chem. Soc.* **1978**, *100*, 1298.

(13) Mitchell, G. R.; King, N. R. *Macromol. Symp.* **1999**, *137*, 155.

(14) Nakahara, H.; Fukuda, K.; Shimomura, M.; Kunitake, T. *Nippon Kagaku Kaishi* **1988**, *7*, 1001.

(15) Itaya, K.; Ataka, T.; Toshima, S. *J. Am. Chem. Soc.* **1982**, *104*, 4767.

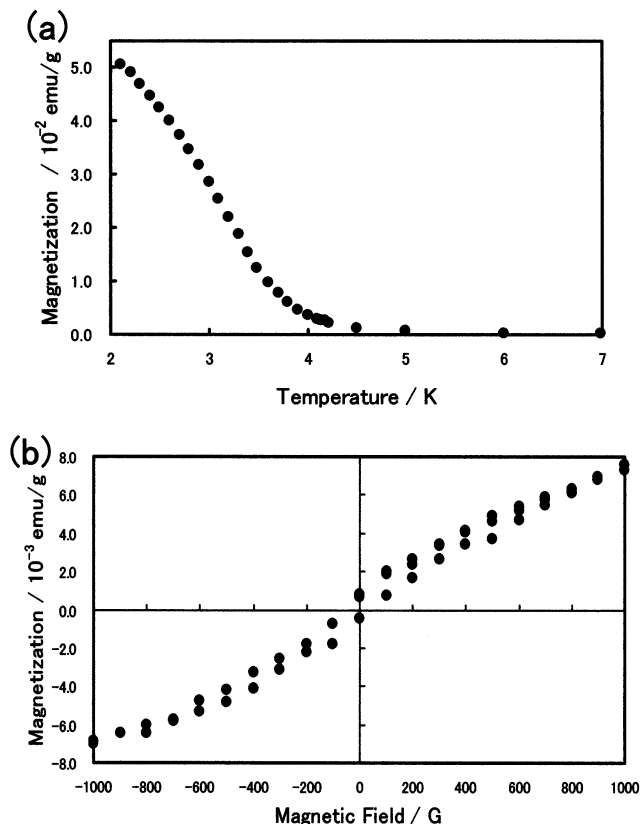


**Figure 5.** (a) Field-cooled magnetization curve with an external magnetic field of 10 G for **2**–Fe–(CN)<sub>6</sub>–Fe. This film exhibits ferromagnetic properties with a critical temperature ( $T_c$ ) of 4.2 K. (b) Hysteresis loop for **2**–Fe–(CN)<sub>6</sub>–Fe at 3 K.

**Photoswitching of Magnetization.** In Figure 5a we show the field-cooled magnetization curve at an external magnetic field of 10 G for the trans form of the **2**–Fe–(CN)<sub>6</sub>–Fe film, which exhibits ferromagnetic properties with a critical temperature ( $T_c$ ) of 4.2 K. This  $T_c$  value is almost identical to that of bulk Prussian blue.<sup>17</sup> A magnetic hysteresis loop was also observed for the film at 3 K, which exhibits a ferromagnetic trend (Figure 5b). The magnetic coupling between the spins of the Prussian blue is explained by a superexchange mechanism involving the ligand orbitals, i.e., the  $\sigma$ -orbital, the  $\pi$ -orbital, and the orthogonal  $\pi$ -orbital of CN.<sup>18,19</sup> The coupling is due to the superexchange interactions through these orbitals. The charge transfer from the occupied  $\pi$ -orbital of the CN bridge to the d-orbital of Fe(II) generates an unpaired electron in the  $\pi$ -orbital, which interacts with the unpaired d-electron of Fe(III). If the orbital overlap between the open-shell  $\pi$ - and d-orbitals is not zero, this orbital-overlap term leads to the nonzero stabilization of the singlet state, namely, the effective superexchange integral is negative (anti-ferromagnetic). On the other hand, if these radical orbitals are orthogonal, the potential exchange term becomes predominant in the charge-transfer configuration, leading to a ferromagnetic superexchange inter-

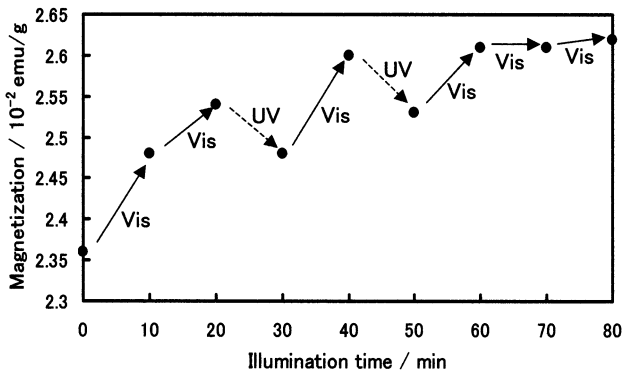


**Figure 6.** Changes and increases in magnetization for film **2**–Fe–(CN)<sub>6</sub>–Fe by visible and UV light illumination at 3 K with an external magnetic field of 10 G. During each step, the illumination was maintained for 10 min. Visible light and UV light were illuminated as indicated in the figure.

action via the Coulombic potential, and therefore the effective superexchange integral is positive.

We observed the influence of light illumination on the magnetic properties of the film as follows. The initial trans state of the **2**–Fe–(CN)<sub>6</sub>–Fe film was cooled to 3 K in a SQUID magnetometer. The initial magnetization value was  $2.35 \times 10^{-2}$  emu/g. During illumination with visible light (400–700 nm, power  $\approx 1.0$  mW/cm<sup>2</sup>, 3 min), the magnetization value increased from  $2.35 \times 10^{-2}$  to  $2.39 \times 10^{-2}$  emu/g. Even after the illumination was stopped, this enhanced magnetization was maintained for at least several hours. The film was then illuminated with UV light (360 nm, power  $\approx 1.0$  mW/cm<sup>2</sup>) for a further 3 min. The degree of magnetization then decreased back to the initial value ( $2.35 \times 10^{-2}$  emu/g). This visible light-induced increase and UV light-induced decrease in the level of magnetization was repeated several times. Although all of the magnetization values were subject to small errors ( $\sim 0.2\%$ ), due to the experimental conditions and the state of photoisomerization of the film, the tendency for a photoinduced increase and decrease in the levels was still reproducible.

When a **2**–Fe–(CN)<sub>6</sub>–Fe film was prepared without washing during the stepwise synthesis process, bulk Prussian blue was formed *outside* the vesicles, and photoillumination did not produce any changes in the total magnetization. This result suggests that the photoillumination affects only the Prussian blue intercalated inside the vesicles. Furthermore, there was no photoillumination effect in the bulk Prussian blue, i.e., without the photoisomerizing bilayer membrane. On the basis of the above results, we have concluded that the magnetization control induced by light illumination is due to the photoisomerization of the bilayer membrane.

**Large Changes in the Magnetic Properties due to Photoillumination.** Next, we investigated how much the photoinduced magnetization might be expected to increase by using a longer duration photoillumination (Figure 6). Six times 10 minutes illumination with visible light and two times 10 minutes illumination with UV light were performed at 3 K. Extended illumination with visible light did not produce further increases in the magnetization, i.e., the photoinduced magnetization changes saturated at around  $2.62 \times 10^{-2}$  emu/g. The total photoinduced increase in the magnetization was ca. 13%, which is much larger

(16) Robin, M. B. *Inorg. Chem.* **1962**, *1*, 337.  
 (17) Ito, A.; Suenaga, M.; Ono, K. *J. Chem. Phys.* **1968**, *48*, 3597.  
 (18) Nishino, M.; Kubo, S.; Yoshida Y.; Nakamura, A.; Yamaguchi, K. *Mol. Cryst. Liq. Cryst.* **1997**, *305*, 109.  
 (19) Klenze, R.; Kanellakopoulos, B.; Trageser, G.; Eysel, H. H. *J. Chem. Phys.* **1980**, *72*, 5819.

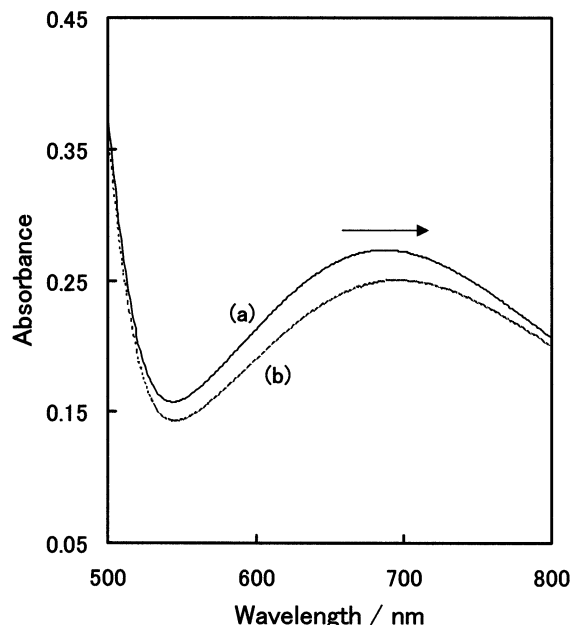


**Figure 7.** Optical absorption spectra of **2**–Fe–(CN)<sub>6</sub>–Fe film (a) before illumination and (b) after 30 min. visible light illumination.

than that achieved by our previous system ( $\sim 1\%$ ), which contained the double-chain ammonium amphiphile.<sup>7</sup> In the present system, the existence of a strong interaction between the chromophores in the vesicle conformation is important. It may restrict the conformation change to some extent, and this is consistent with the experimental results that show the UV–Vis absorption spectra change (Figure 3c). Thus, the UV-light induced decrease in the magnetization shown in Figure 6 was not perfect because the solid-state photochromic reaction is greatly inhibited by the close packing of the chromophores. Also, nonperfect reversibility suggested that a whole composite material with cis form was a little more stabilized thermodynamically than that with trans form because of the close packing, although the mechanisms are not clear at present. Although only a large photoinduced increase in the magnetization was observed in the present experiment, it is expected that we can switch the magnetization reversibly by at least 10% by an extended (more than 60 min) visible–UV illumination.

The most significant difference from the previous system<sup>7</sup> is that the photofunctional vesicles consist of only the azo moiety. Basically, just as with the previous system, it is proposed that photoisomerization of the film is accompanied by a geometrically confined structural change, as reflected by the changes in the dipole moment and the electrostatic field. The very small change ( $\sim 1\%$ ) in the magnetization induced by photo-illumination in the previous system was due to the small interaction between the azo moiety and the magnetic materials (Prussian blue). This was because the azo moiety was diluted by the double-chain ammonium amphiphile and therefore the interaction between the chromophores was similar to that in the solution.

On the other hand, it is suggested that the change in the dipole moment and the electrostatic field caused by photoisomerization was large in the present system, because only the azo moiety **1** formed the spherical

vesicles by itself, in a regular layered structure. In addition to this, the interaction between the azo moiety and the magnetic material (Prussian blue) is stronger because the amphiphilic bilayers have an ion exchangeable site ( $-\text{SO}_3^- \text{Na}^+$ ) close to the azo moiety, and so the surface of the Prussian blue might be coordinated close to the azo moiety.

Generally, the main absorption band of the azobenzene chromophore is the  $\pi-\pi^*$  band, for which the transition dipole is directed along the long axis of the azo moiety.<sup>20</sup> Photoinduced reorientation has been observed with azobenzenes in various forms of molecular organization, such as in LB films or in liquid-crystalline side-chain polymers. The mechanism for the reorientation is also well understood.<sup>21,22</sup> Photoisomerization from the trans to cis forms, with a subsequent thermal or photoassisted isomerization back to the trans form, may lead to a change in the orientation of an individual chromophore.

As mentioned before, for Prussian blue intercalated into films **2**, the absorption maximum,  $\lambda_{\text{max}}$  (internal charge-transfer band from Fe<sup>II</sup> to Fe<sup>III</sup>), was observed at 680 nm, which is blue-shifted by ca. 20 nm from that of bulk Prussian blue. However, the  $\lambda_{\text{max}}$  peak of the films after 30 min illumination (i.e., after trans-to-cis photoisomerization) was shifted to 700 nm, which is almost the same as that of bulk Prussian blue (Figure 7). The existing electrostatic field lowers the Coulombic energy necessary for transferring an electron from the hexacyanoferrate (II) ion to the surface Fe (III) species of the intercalated Prussian blue by the effect of the illumination. On the other hand, the shift in  $\lambda_{\text{max}}$  after the illumination was undetectable in the case of our previous system. These results are consistent with the large change in the magnetic properties in the present system. As mentioned before, the magnetic coupling between spins of the Prussian blue can be explained by a superexchange mechanism involving the ligand orbitals of the CN. When the orbitals are orthogonal, the potential exchange term becomes predominant in the charge-transfer configuration, leading to a ferromagnetic superexchange interaction via the Coulombic potential. Namely, the effective superexchange integral is positive. It is suggested that the change in the Coulombic energy necessary to transfer an electron from the hexacyanoferrate (II) ion to the surface Fe (III) species might affect the superexchange interaction between the spins in the Prussian blue magnet.

## Summary

We have succeeded in preparing a new material for photofunctional magnetic vesicles. The present work proved that such a strategy for preparing inorganic/organic composite materials was quite effective for designing novel photofunctional systems. Furthermore, it is expected that a reversible photoswitching of magnetization *with a large value at higher temperature* is possible by designing an appropriate system.

CM020713B

(20) Schönhoff, M.; Mertesdorf, M.; Lösche, M. *J. Phys. Chem.* **1996**, *100*, 7558.

(21) Möbius, G.; Pietsch, U.; Geue, T.; Stumpe, J.; Schuster, A.; Ringsdorf, H. *Thin Solid Films* **1994**, *247*, 235.

(22) Manzel, H.; Weichert, B.; Schmidt, A.; Paul, S.; Knoll, W.; Stumpe, J.; Fischer, T. *Langmuir* **1994**, *10*, 1926.